

Contents

1	LPOTT: Simulation of Pion-Nucleus Scattering, 8/02	3
1.1	Introduction	3
1.1.1	Thumbnail Sketch of Lab	3
1.1.2	Learning Goals	3
1.1.3	Why Need High Performance Computing	3
1.1.4	Purpose of this Research	4
1.1.5	Computer Language	4
1.1.6	Required Resources	4
1.2	Physics Background	4
1.2.1	Scattering Kinematics	5
1.2.2	Scattering Cross Sections	7
1.2.3	Scattering Wave Functions	8
1.2.4	Partial Waves	9
1.2.5	Resonances and Argand Plots	10
1.2.6	Coulomb-Nuclear Interference	11
1.2.7	The Optical Potential	11
1.2.8	Schrödinger Equation to be Solved	13
1.2.9	Solution via Inversion or Elimination	14
1.3	Simulation: Get LPOTT Running	15
1.3.1	Compiling	15
1.3.2	Understanding the Output	16
1.3.3	Understanding the Logic: Follow the Data Flow	18
1.4	Experiments	18
1.4.1	Experiment 1: Checking the Input π N Scattering	18
1.5	Experiment 2: Low-Energy $\pi - {}^4\text{He}$ Scattering	21
1.6	Experiment 3: Pion-Nucleus Total Cross Sections	23
1.7	Experiment 4: P33 Resonance in $\pi^- - {}^{12}\text{C}$ Scattering	25
1.8	Experiment 5: Make a Nucleus Black	26
1.9	Reprints of Original Papers	28
	October 1, 2002	

Chapter 1

LPOTT: Simulation of Pion-Nucleus Scattering, 8/02

1.1 Introduction

1.1.1 Thumbnail Sketch of Lab

The program LPOTT[LPOTT] simulates the multiple scattering of a pion by the various nucleons within a nucleus. You give LPOTT¹ the energy of the pion incident on specified target nucleus, and it computes the scattering cross sections and wave functions. LPOTT solves an integral equation in momentum space that is just the Schrödinger equation specialized for scattering. This integral equation is reduced to simultaneous linear equations which are solved with matrix techniques. The physics investigated includes the effect of the pion-nucleon resonances, the interference of Coulomb and nuclear forces, and the multiple scattering of the pion within the nucleus. Further studies include the focusing of the pion's wave function caused by an absorptive nucleus and the importance of nuclear spin flip.

1.1.2 Learning Goals

- understanding how the many-body nature of the nucleus affects the scattering
- gaining experience with the solution of integral equations
- gaining experience with matrix equations and matrix manipulations
- understanding how interpolation on a data set converts it into a function
- understanding the physics of scattering

1.1.3 Why Need High Performance Computing

Since LPOTT solves the Schrödinger equation as an integral equation in momentum (Fourier) space, it requires more computing time than solving a differential equation. When the first versions of LPOTT were written in 1972, it was revolutionary in its promise to provide a more precise description of nuclear scattering than was possible by doing the calculation in \mathbf{r} space. While LPOTT lived up to its promise, the fact that it took 10-100 times longer to perform the calculation than the standard coordinate-space codes meant that it was considered very “expensive” to run. That was a time when computers were thousands of times slower than today, and when computer time was so precious that researchers had to buy every second of it (one hour of computer time cost about the same as one month of

¹LPOTT is an acronym of sorts for the Landau-Phatak-Tabakin Optical Potential.

graduate student salary). Although there are thousands of lines of Fortran code in LPOTT, modern computers are so fast that running time is no longer an issue.

When LPOTT was used as an instrument for basic research, it was important to test the sensitivity of the calculation to various theoretical assumptions, as well as to the parameters used to describe the nuclear size and shape. For these reasons there are a bunch of numbers that the user “feeds” LPOTT to get it going. Some of these *input data* are “switches” that control the logical flow within the calculation, while others are parameters that give the size and shape of the nucleus or control different aspect of the interaction.

1.1.4 Purpose of this Research

- to learn about the structure of nuclei via π scattering
- to understand the mechanism of how a π interacts with a nucleus
- to learn about the pion-nucleon (πN) interaction via π scattering from the collection of nucleons within a nucleus

1.1.5 Computer Language

Fortran 77.

1.1.6 Required Resources

disk space, Ram, file sizes, CPU time.

1.2 Physics Background

The scattering of a π by a nucleus arises from the nuclear (or strong) and Coulomb forces between a π and the nucleus of an atom in the target. This force may be attractive or repulsive, and, indeed, you will conduct an experiment to determine which it is. Yet even if the nuclear force were infinitely attractive, angular momentum conservations requires that the incident beam will be scattered from the nucleus and not captured by it. For the high energies considered in this lab (millions of electron volts), we can safely ignore any scattering from electrons in the target and consider just the nuclei.

Before we plow into the theory, it is important to understand what pions are, why they occur in nature, and why anyone would want to smash them into a nucleus. The π story begins in 1935 when Yukawa[Yuk35] discovered that quantum field theory could be used to provide the first theoretical description of the nuclear and short-ranged force between the neutrons and protons (“nucleons”) in the nucleus. To accomplish this, Yukawa postulated that the nuclear force arises when one N emits a particle that is subsequently absorbed by a different N. To get the nucleons to fit inside the small size of a nucleus ($\Delta x \sim 10^{-13}cm$) and still satisfy the uncertainty principle $\Delta x \Delta p \simeq \hbar$. Yukawa realized that the exchanged particle had to have a mass of about 1/7th that of a N. Although it took some years for this particle to be found, we now call it the π meson or *pion*. (The term “meson” denotes particles that are intermediate in mass between heavy ones like nucleons, and light ones like electrons).

While pions are the strong glue that holds nuclei together, when removed from a nucleus and placed in free space, they are unstable and decay with a mean lifetime of 3×10^{-8} seconds. Because they have such short lifetimes, it has been a challenge to determine the properties of isolated pions as well as the nature of their interactions with other particles. The pions don’t live long enough to be placed in an accelerator, nor to make a target out of them. However, an accelerator can produce protons with such high energies that when they hit a “production” target, some of the proton’s kinetic energy is converted into pions, and a beam of pions is produced. If a secondary target is placed nearby, some of these pions will

hit that target and interact with the nuclei within the target. This is what we simulate in the present lab.

Once we have the ability to form a beam of pions, we smash them into nuclei to learn more about the nucleus or about the π and its interactions. Pions are a particularly useful probe of nuclei since their unique properties make them sensitive to different aspects of the nucleus than other probes, and thereby able to view the nucleus “in a different light”. We also study the interaction of pions with nuclei to learn about π interactions that are otherwise impossible to observe. For example, neutrons are too unstable to be made into a target to scatter from, yet the neutrons inside of a nucleus are stable and can thereby be used to study π -neutron scattering (two unstable particles).

1.2.1 Scattering Kinematics

In a scattering experiment a beam of particles of well-defined momentum is directed at a target (often a thin foil). Unless the target is very thick, most of the beam passes through the target undeflected with some small number of particles scattered out of the beam at various angles. The measurements made in a scattering experiment are of the number of particles and their energies scattered at each angle.

In Fig. 1.1 we show a schematic diagram of a typical scattering experiment. The beam comes in from the left and moves along the positive z axis to the right. The target is at the origin, and a scattered particle is observed at a polar scattering angle θ and an azimuthal angle ϕ . If, as we assume for this lab, the force between the beam particle and the target particle is *central*, that is, lies along the line connecting the centers of the two particles, then rotational invariance demands that the scattering not depend upon the azimuthal angle ϕ .

The laboratory frame of reference, or “lab frame” is the reference frame in which the target particle is initially at rest. While experiments are conducted in the lab frame, it is easier to understand the physics of scattering in the center-of-momentum (COM) reference frame. As we show in Fig. 1.2, the COM frame is the one in which a particle in the beam and a particle in the target have equal and opposite momenta.

In this lab we compute the *elastic* scattering of pions from a nucleus, that is, scattering in which no internal degrees of freedom are excited. We perform the calculation in the π -nucleus COM frame where the theory is simplest, but then relate it to quantities in the lab frame, where the measurements are made. As we see in Fig.??, this means that in the COM, the scattering process consists of just a rotation of the initial momenta of the beam and target into the final momenta[QMII].

For nonrelativistic scattering, the momentum transfer \mathbf{q} is the same in the lab and COM frames:

$$\mathbf{q} = \mathbf{p}'_{lab} - \mathbf{p}_{lab} = \mathbf{k}' - \mathbf{k}, \quad (1.1)$$

where a prime is used to denote momenta after the scattering, and \mathbf{k} is used to denote momenta in the COM. For relativistic scattering, the kinematic relations are based on the Lorentz invariance of the COM energy or its square s :

$$E_{COM} = E_P(k) + E_T(k) = \sqrt{M_P^2 + k^2} + \sqrt{m_T^2 + k^2} = \sqrt{s}, \quad (1.2)$$

$$\Rightarrow k^2 = \frac{[s - (m_P + m_T)^2][s - (m_P - m_T)^2]}{4s}. \quad (1.3)$$

Here the subscripts P and T denote projectile and target respectively. Since s is a relativistic invariant, it can be evaluated in the lab as well,

$$s = m_P^2 + m_T^2 + 2m_T E_P(p_{lab}), \quad (1.4)$$

$$\Rightarrow \mathbf{p}_{lab} = \frac{\mathbf{k}\sqrt{s}}{m_P}. \quad (1.5)$$

This means that knowing the COM energy s gives the COM momentum k , as well as the lab momentum P_{lab} .

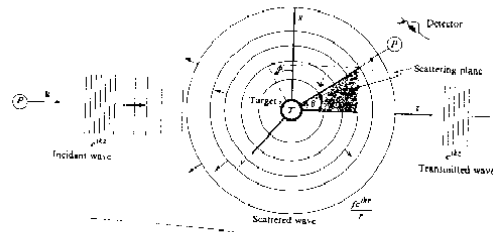


Figure 1.1: The incident, scattered, and transmitted waves in a scattering experiment. \mathbf{k} and \mathbf{k}' are the initial and final projectile momenta θ is the scattering angle.

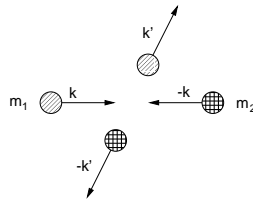


Figure 1.2: The elastic scattering of mass m_1 and m_2 in their center-of-momentum system. Only the direction of the momenta change.

If we know the COM energy, we can determine the π lab energy and momentum via

$$E_{\pi}^{lab} = \frac{E_{cm}^2 - m_{\pi}^2 - m_N^2}{2m_N}, \quad (1.6)$$

$$T_{\pi} = E_{\pi}^{lab} - m_{\pi}^2, \quad (1.7)$$

$$p_{\pi} = \sqrt{E_{\pi} - m_{\pi}^2}. \quad (1.8)$$

1.2.2 Scattering Cross Sections

In a scattering experiment, such as that sketched in Fig. 1.1, the experimentalist counts the number of particles scattered into their detector located at some angle θ and ϕ . Usually, the results of a scattering experiment are converted into the scattering cross section $\sigma(\theta, \phi)$ that is a function of the scattering angle. For scattering into the differential solid angle $d\Omega = d\cos\theta d\phi$, we deal with the differential cross section per unit solid angle, $d\sigma/d\Omega$. Cross sections are independent of the details of the experimental apparatus, independent of the intensity of the incident beam, independent of the amount of target material, and of the size of the detector. This is what makes them universal.

The differential cross section for elastic scattering $d\sigma/d\Omega$ is defined with reference to the scattering setup of Fig. 1.1,

$$\frac{d\sigma}{d\Omega}(\theta, \phi) = \lim_{\Delta \rightarrow 0} \frac{N(\theta, \phi)/\Delta\Omega}{N_{in}/\Delta A_{in}}. \quad (1.9)$$

That is, to obtain a quantity independent of detector size, we divide the number of particles scattered into the detector N , by the solid angle subtended by the detector $\Delta\Omega$, and then take the limit for infinitesimally small detector size and infinitesimally thin targets.

It follows from (1.20) that $d\sigma/d\Omega$ has the dimension of area, or area per solid angle (per steradian). For nuclear scattering, a natural unit is Fermi²/steradian or millibarn/steradian. Note that 1 Fermi = 10^{-13} cm \equiv 1 fm, 1 barn = 10^{-24} cm², and 1 millibarn \equiv mb = fm²/10. (The *Barn* is a very large unit; for most nuclear processes it is so large that a target producing a cross section of a Barn would be as easy to hit as “the broad side of a barn.”)

Classically, the cross section σ is the effective cross sectional area the target presents to the beam. Indeed, $\sigma = \pi R^2$ for a hard sphere target of radius R . The quantum-mechanical cross section describes the scattering of waves, and much like the scattering of light waves, often varies rapidly with energy and angle. The analogy is so strong that the literature of scattering theory borrows optical terms such as diffraction, dispersion, absorption, interference, and index of refraction.

In elastic scattering the cross section as measured in the COM and lab frames are related by

$$\left. \frac{d\sigma}{d\Omega}(\theta, \phi) \right|_{lab} = \left. \frac{d\sigma}{d\Omega}(\theta, \phi) \right|_{COM} \frac{d(\cos\theta)}{d(\cos\theta_{lab})}, \quad (1.10)$$

where angles without subscripts are in the COM. For nonrelativistic collisions, the lab and COM scattering angles are related by

$$\tan\theta_{lab} = \frac{\sin\theta}{\cos\theta + m_P/m_T}. \quad (1.11)$$

For relativistic collisions, we invoke the Lorentz invariance of the square of the 4-momentum transfer,

$$t = (p'_P - p_P)^2 = (p'_T - p_T)^2, \quad (1.12)$$

evaluate t in both frames, and obtain the relation between the scattering angles,

$$\cos\theta = \frac{E_P(k)^2 - E_P(p_{lab})E_P(p'_{lab}) + p_{lab}p'_{lab}\cos\theta_{lab}}{k^2}, \quad (1.13)$$

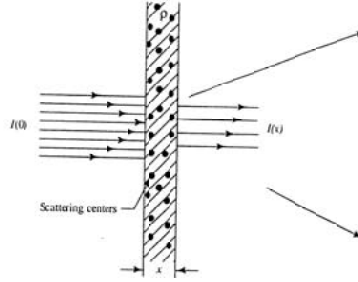


Figure 1.3: A setup for measuring a total cross section by observing the depletion of a beam's intensity from $I(0)$ before the target to $I(x)$ after the target.

where the prime is used to denote the scattered or final particle.

The *total cross section* is just integrated elastic cross section:

$$\sigma_{\text{el}} = \int d\Omega \frac{d\sigma}{d\Omega} = \int_0^{2\pi} d\phi \int_{-1}^1 d(\cos\theta) \frac{d\sigma}{d\Omega}(\theta). \quad (1.14)$$

Total cross sections can be measured very simply by just passing a beam of intensity I_0 through a target of thickness t as shown in Fig. 1.3. If you also measure the intensity I of the beam when it leaves the target, the two intensities are related by

$$I = I_0 e^{-\sigma \rho t}, \quad (1.15)$$

where ρ is the density of the target.

1.2.3 Scattering Wave Functions

Our time-independent view of the scattering experiment is shown in Fig. 1.1. We describe the incident beam as a plane wave² continuously entering along the negative z axis:

$$\phi_{\mathbf{k}}(\mathbf{r}) = \frac{1}{(2\pi)^{3/2}} e^{i\mathbf{k}\cdot\mathbf{r}} = \frac{1}{(2\pi)^{3/2}} e^{ikz}, \quad (1.16)$$

where the subscript \mathbf{k} indicates the beam's momentum. The constant $1/(2\pi)^{3/2}$ in these equations is a normalization factor chosen to provide delta-function normalization of the plane wave.

The complete scattering setup in Fig. 1.1 is described by there being a plane wave plus a scattered wave:

$$\psi_{\mathbf{k}}(\mathbf{r}) = \phi_{\mathbf{k}}(\mathbf{r}) + \psi_{\mathbf{k}}^{\text{SC}}(\mathbf{r}). \quad (1.17)$$

Here the scattered wave $\psi_{\mathbf{k}}^{\text{SC}}(\mathbf{r})$ describes the scattered particles radiating away from the target. A spherical, radiating wave has the form

$$\psi_{\mathbf{k}}^{\text{SC}}(\mathbf{r}) \sim f_E(\theta, \phi) \frac{e^{ikr}}{r}, \quad (1.18)$$

where $f_E(\theta, \phi)$ is the amplitude of the scattered wave, or as the *scattering amplitude*. The complete wave function accordingly has the asymptotic form

$$\psi_{\mathbf{k}}(\mathbf{r}) \sim \frac{1}{(2\pi)^{3/2}} \left[e^{ikz} + f_E(\theta, \phi) \frac{e^{ikr}}{r} \right]. \quad (1.19)$$

²So called because it occupies an infinite 2D plane in space.

A crucial result of scattering theory is that the scattering amplitude $f_E(\theta, \phi)$ can be determined experimentally by measuring cross sections. Specifically for elastic scattering, the differential cross section is just the squared modulus of the scattering amplitude:

$$\frac{d\sigma}{d\Omega}(\theta, \phi) = |f_E(\theta, \phi)|^2. \quad (1.20)$$

1.2.4 Partial Waves

While a plane wave is a reasonable model for the incident beam in a scattering experiment, the mathematical analysis becomes simpler if the incident beam were a spherical wave. We take advantage of this simplicity and the law of linear superposition by decomposing the incident plane wave into the sum of an infinite number of spherical, *partial waves*:

$$\phi_{\mathbf{k}}(\mathbf{r}) = \frac{e^{i\mathbf{k}\cdot\mathbf{r}}}{(2\pi)^{3/2}} = \sum_{l=0}^{\infty} \frac{(2l+1)i^l j_l(kr) P_l(\cos\theta)}{(2\pi)^{3/2}}. \quad (1.21)$$

Here $P_l(\cos\theta)$ is the Legendre polynomial and $j_l(kr)$ is the spherical Bessel function. The combination of incident and scattering wave make up the complete wave function of the system and is also expanded as the sum of partial waves

$$\psi_{\mathbf{k}}(\mathbf{r}) = \sum_{l=0}^{\infty} \frac{(2l+1)i^l P_l(\cos\theta) u_l(kr)}{kr(2\pi)^{3/2}}, \quad (1.22)$$

where we must solve for the radial wave function $u_l(kr)$. The u_l 's are called distorted partial waves and are related to the scattering phase shifts via their behavior at large r :

$$u_l(kr) \sim e^{i\delta_l(E)} [\sin \delta_l \cos(kr - l\pi/2) + \cos \delta_l \sin(kr - l\pi/2)] \quad (1.23)$$

$$= e^{i\delta_l} \sin(kr - l\pi/2 + \delta_l). \quad (1.24)$$

In turn, the phase shifts are related to the scattering amplitude that can be measured by experiment:

$$f_E(\theta) = \sum_{l=0}^{\infty} (2l+1) P_l(\cos\theta) \frac{(\eta_l e^{2i\delta_l} - 1)}{2ik}, \quad (1.25)$$

$$= \sum_{l=0}^{\infty} (2l+1) P_l(\cos\theta) \frac{T_l(k)}{k}, \quad (1.26)$$

$$T_l(k) = \frac{(\eta_l e^{2i\delta_l} - 1)}{2i}. \quad (1.27)$$

Here $T_l(k)$ is called the partial wave amplitude, and has the $1/k$ factor removed from it to leave it with unit modulus. In terms of these amplitudes, the total cross section is:

$$\sigma^{tot} = \frac{4\pi}{k^2} \sum_{l=0}^{\infty} (2l+1) \text{Im} T_l. \quad (1.28)$$

For the scattering that we simulate in this lab, the nucleus has the capability not only of scattering the incident waves on it, but also of actually *absorbing* some of that wave so that they effectively disappear (like light being absorbed by a cloudy mirror). For cases such as these, the *absorption parameter* in (1.27) $\eta_l \leq 1$. For elastic scattering, $\eta_l = 1$.

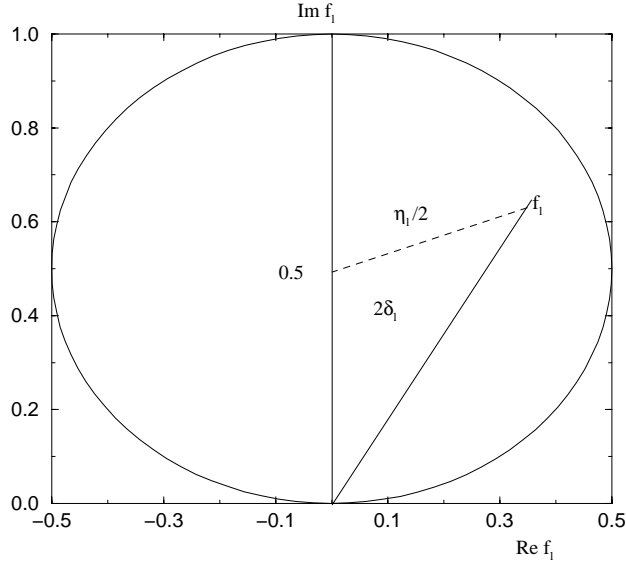


Figure 1.4: The parameters involved in an Argand diagram and their geometrical interpretation: the central angle is $2\delta_l$, the absorption parameter η_l is the radius, and determines the complex amplitude T_l .

1.2.5 Resonances and Argand Plots

Resonances occur when sound waves get stuck in organ pipes and when quantum waves get stuck in potential wells. They also occur when strongly interacting particles get so close to each other that they bind for short times. One of the things that makes this lab interesting is that the input π -N system has a very strong resonance in the $l = 1$ partial wave. This resonance is called the $P_{3/2,3/2}$ resonance or $P33$ for short. The P denotes an orbital angular momentum $l = 1$ state, the first $3/2$ indicates that this is an isospin $3/2$ state, and the second $3/2$ indicates that the total angular momentum $j = l + s = 3/2$.

At the resonance energy for a potential resonance, the imaginary part of the scattering amplitude has a maximum, the real part of the amplitude has a zero, and the scattering phase shift $\delta = \pi/2$. Since the optical theorem relates the total cross section to the imaginary part of the forward scattering amplitude via

$$\sigma_{tot} = \frac{4\pi}{k} \text{Im}f(\theta = 0), \quad (1.29)$$

the maximum in $\text{Im}f(0)$ leads to a maximum of the scattering cross section at the resonance energy also.

One way of visualizing resonances is to draw the partial wave scattering amplitude as an *Argand diagram* as in Fig. (1.4). This is a parametric plot of the imaginary part of the scattering amplitude versus the real part. This is parametric because both $\text{Im}T_l$ and $\text{Re}T_l$ are functions of the energy E , which is the parameter, yet does not appear explicitly in the plots. For each energy, we evaluate $\text{Im}T_l$ and $\text{Re}T_l$, and then get one point on the diagram.

The scale in an Argand diagrams is usually set by drawing a unit-diameter circle centered at $(0, 1/2)$. If we look at the expression (1.27) for the partial wave scattering amplitude, we see that we can relate the phase shift δ and absorption parameter η_l to each point in the Argand plot. If we draw a line from the origin to a point, the angle the line makes with the vertical is 2δ , and the distance from the center of the circle to a point is $\eta_l/2$.

The visualization value of these diagrams becomes clear when a resonance occurs, that is, when the phase shift δ increases rapidly through $\pi/2$ a function of energy. This is seen on the Argand plot as a point moving counterclockwise on the circle as a function of energy and passing through the vertical at the resonance energy. If the resonance is *inelastic* with $\eta_l < 1$, then there is still a loop, but its shape gets distorted.

1.2.6 Coulomb-Nuclear Interference

As a charged π scatters from a nucleus, it is affected by both Coulomb and nuclear forces. Since there is no way of separating the effects of these forces, we follow the quantum prescription of adding the corresponding Coulomb and nuclear scattering amplitudes [QMII]:

$$f(\theta) = f_c^{\text{pt}}(\theta) + f_{NC}(\theta). \quad (1.30)$$

Here f_c^{pt} is the scattering amplitude that would arise if there were solely scattering from a point Coulomb charge:

$$f_c^{\text{pt}} = -\frac{\gamma}{2k_0 \sin^2 \theta/2} \exp(2i\sigma_0 - \gamma \ln \sin^2 \theta/2), \quad (1.31)$$

where γ is the Coulomb parameter (positive for a repulsive interaction),

$$\gamma = \frac{Z_T Z_P e^2}{v}, \quad (1.32)$$

with v the target-projectile relative velocity, and Z_P and Z_T the projectile and target charge numbers. The function f_{NC} in (1.30) is the scattering amplitude arising from the nuclear scattering of a wave that has been distorted by the Coulomb force:

$$f_{NC}(\theta) = \frac{1}{ik_0} \sum_{l=0}^{\infty} (2l+1) e^{2i\sigma_l} [e_l^{2i\delta^{NC}} - 1] P_l(\cos \theta), \quad (1.33)$$

where the extra phase, $\sigma_l = \arg \Gamma(l+1+i\gamma)$, accounts for the Coulomb distortion of the incident wave. As usual, the differential cross section is formed by forming the squared magnitude of the scattering amplitude:

$$\frac{d\sigma}{d\Omega} = |f(\theta)|^2. \quad (1.34)$$

1.2.7 The Optical Potential

Although you would be correct to suspect that the passage of a strongly-interacting particle through a nucleus is complicated, it is successfully modelled as an analog to the passage of a light wave through a cloudy crystal ball. Some of the wave gets refracted (bent) and some of it gets diffracted (absorbed). So when you make the π interaction strong enough in the simulation, you will see that the nucleus appears as a “black disk” to the π , with a characteristic large forward peak followed by a number of diffraction minima.

The technique we use to model the passage of pions through nuclei is to solve the Schrödinger equation with a potential that has the properties of a cloudy crystal ball. In particular, the potential has an imaginary part to account for the absorption of pions by the nucleus, an energy dependence to account for the energy dependence of the elementary π interaction, and a *nonlocality* to account for the fact that while the π may be interacting with one N, that N may be interacting with other nucleons at other places in the nucleus. This kind of potential is called an *optical potential* in analogy to the passage of light through a cloudy crystal ball. By solving the Schrödinger equation in momentum space, we include the proper nonlocalities and energy-momentum dependences of the optical potential that would otherwise be lost if transformed to coordinate space.

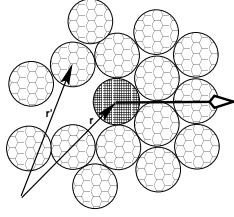


Figure 1.5: A pion in the lower left of the figure is interacting with a nucleon at \mathbf{r} (dark sphere). As a consequence of interactions with nearby nucleons at \mathbf{r}' , the potential that the pion feels is nonlocal, that is, $V(\mathbf{r}, \mathbf{r}')$.

The formula for the optical potential can be derived via a simple, intuitive argument. Consider Fig. 1.2.7 showing the nucleons within a nucleus (shaded spheres) that the π (white sphere) interacts with when it enters the nucleus. In order for the π to interact with the nucleus in some region of space, there must be nucleons present nearby. The probability of finding nucleons in some region of space is given by the average nuclear density $\rho(r)$. Accordingly, the optical potential U is proportional to ρ :

$$U(r) \propto \rho(r). \quad (1.35)$$

In some region of space where there are nucleons, the strength of the π 's interaction with the nuclear medium is proportional to the strength of the π 's interaction with an individual N. The measure of the strength of this interaction is given by the π -N scattering amplitude $f_{\pi N}$ or T matrix $t_{\pi N}$ (the two are proportional):

$$U(r) \propto t_{\pi N}(r)\rho(r). \quad (1.36)$$

We note that the size of the nucleus enters the potential through $\rho(r)$, while the size of the elementary π -N interaction enters via the r -dependence of $t_{\pi N}(r)$ (which we Fourier transform into $t_{\pi N}(k)$).

A more rigorous derivation[KMT] determines the optical potential in momentum (Fourier transform) space to be:

$$\langle \mathbf{k}' | V | \mathbf{k} \rangle = -\frac{4\pi}{k} \langle \mathbf{k}' | t_{\pi N} | \mathbf{b}\mathbf{k} \rangle \tilde{\rho}(\mathbf{k}' - \mathbf{k}). \quad (1.37)$$

The t in this equation is T matrices, and is just a generalization of the scattering amplitude to cases where the initial and final COM momenta differ³. When the initial and final momenta have the same magnitude, we have what is known as “on-energy-shell” scattering, and the T matrix becomes proportional to the scattering amplitude:

$$f_E(\theta, \phi) = -4\pi^2 \mu T_E(\mathbf{k}', \mathbf{k}) \Big|_{k'=k}, \quad (1.38)$$

where μ is a reduced mass.

The function $\tilde{\rho}(\mathbf{k}' - \mathbf{k})$ in (1.37) is the Fourier transform of the nuclear density $\rho(r)$ that was introduced in (1.36):

$$\tilde{\rho}(\mathbf{k}' - \mathbf{k}) = \int d\mathbf{r} e^{i(\mathbf{k}' - \mathbf{k}) \cdot \mathbf{r}} \rho(r). \quad (1.39)$$

$\tilde{\rho}(\mathbf{k}' - \mathbf{k})$ is called the *nuclear form factor* and contains all the information about the nuclear size and shape that we need for the computation. Since the neutrons and protons within the nucleus may have somewhat different distributions, LPOTT accounts for that by generalizing

³We are formulating this problem with “natural” units in which Planck’s constant $\hbar \equiv 1$. This means that there is no difference between momentum and wave vectors.

the formula for the optical to include separate form factors and T matrices for neutrons and protons:

$$\langle \mathbf{k}' | V | \mathbf{k} \rangle = -\frac{4\pi}{k} [\langle \mathbf{k}' | t_{\pi p} | \mathbf{k} \rangle \tilde{\rho}_p(\mathbf{k}' - \mathbf{k}) + \langle \mathbf{k}' | t_{\pi n} | \mathbf{k} \rangle \tilde{\rho}_n(\mathbf{k}' - \mathbf{k})]. \quad (1.40)$$

1.2.8 Schrödinger Equation to be Solved

Because scattering experiments measure cross sections and scattering amplitudes, it is convenient to convert the Schrödinger equation into an equation dealing with amplitudes rather than wave functions. An integral form of the Schrödinger equation dealing with the amplitude R (reaction matrix) is

$$R(k', k) = V(k', k) + \frac{2}{\pi} \mathcal{P} \int_0^\infty dp \frac{p^2 V(k', p) R(p, k)}{(k_0^2 - p^2)/2\mu}, \quad (1.41)$$

where the symbol \mathcal{P} in (1.41) indicates that the Cauchy principal-value prescription is used to avoid the singularity arising from the zero of the denominator (the R matrix is a simpler version of the T matrix). As is evident from the denominator under the integral, this equation uses the nonrelativistic formula for energy. We use it here to keep the equations simpler even though LPOTT uses the relativistic definition of energy:

$$E(k_0) = \sqrt{m_\pi^2 + k_0^2} + \sqrt{m_A^2 + k_0^2}. \quad (1.42)$$

We solve (1.41) in order to determine the diagonal matrix element $R(k_0, k_0)$. This number determines the experimental scattering phase shift via

$$R(k_0, k_0) = -\frac{\tan \delta_l}{2\mu k_0}, \quad (1.43)$$

where μ is a reduced mass. Even though we may want to compute only the number $R(k_0, k_0)$ since (1.41) is an integral equation it requires an integration of $R(p, k)$ over all p values. Yet since $R(p, k)$ is an unknown, we can't solve for the single number $R(k_0, k_0)$ without also solving for the entire function $R(p, k)$. Accordingly, $R(p, k)$ is solved for all values of p with only the $p = k_0$ piece used to determine the scattering amplitude (we do use the other pieces to compute the wave function).

The technique for solving the integral equation (1.41) is to reduce it to simultaneous linear equations that are then solved with matrix techniques. First we have to transform the Cauchy principal part prescription into something that can be computed. This we do by writing the principal-value prescription as the definite integral:

$$R(k', k) = V(k', k) + \frac{2}{\pi} \int_0^\infty dp \frac{p^2 V(k', p) R(p, k) - k_0^2 V(k', k_0) R(k_0, k)}{(k_0^2 - p^2)/2\mu}. \quad (1.44)$$

We convert the integral equation (1.44) into linear equations by approximating the integral as a sum over N Gaussian quadrature integration points $\{k_j; j = 1, N\}$ with weights w_j :

$$\begin{aligned} R(k, k_0) &\simeq V(k, k_0) + \frac{2}{\pi} \sum_{j=1}^N \frac{k_j^2 V(k, k_j) R(k_j, k_0) w_j}{(k_0^2 - k_j^2)/2\mu} \\ &\quad - \frac{2}{\pi} k_0^2 V(k, k_0) R(k_0, k_0) \sum_{m=1}^N \frac{w_m}{(k_0^2 - k_m^2)/2\mu}. \end{aligned} \quad (1.45)$$

Note here that the last term in (1.45) implements the principal-value prescription and cancels the singular behavior of the first term.

$$\underbrace{R(k_1) \quad R(k_2) \quad R(k_3) \quad \dots \quad R(k_N)}_{\text{Grid in momentum space}}$$

Figure 1.6: The grid in momentum space on which the integral equation for the R is solved.

Equation (1.45) contains the N unknowns $R(k_j, k_0)$, $j = 1, N$, and $R(k_0, k_0)$. We turn this into $N + 1$ simultaneous equations by evaluating it for $N + 1$ k values on the grid shown in Fig. 1.6:

$$k = k_i = \begin{cases} k_j, & j = 1, N \quad (\text{quadrature points}), \\ k_0, & i = 0 \quad (\text{experimental point}). \end{cases} \quad (1.46)$$

There are now $N + 1$ unknowns $R(k_i, k_0) \equiv R_i$, and $N + 1$ linear equations for them:

$$R_i = V_i + \frac{2}{\pi} \sum_{j=1}^N \frac{k_j^2 V_{ij} R_j w_j}{(k_0^2 - k_j^2)/2\mu} - \frac{2}{\pi} k_0^2 V_{ii} R_0 \sum_{m=1}^N \frac{w_m}{(k_0^2 - k_m^2)/2\mu} \quad (i = 1, N + 1). \quad (1.47)$$

We express these equations as a matrix equation by first combining the denominators and weights into a single denominator vector D :

$$D_i = \begin{cases} +\frac{2}{\pi} \frac{w_i k_i^2}{(k_0^2 - k_i^2)/2\mu}, & \text{for } i = 1, N, \\ -\frac{2}{\pi} \sum_{j=1}^N \frac{w_j k_0^2}{(k_0^2 - k_j^2)/2\mu}, & \text{for } i = N + 1. \end{cases} \quad (1.48)$$

The linear equations (1.47) now assume the matrix form

$$[R] = [V] + [DV][R]. \quad (1.49)$$

Here R and V are *column vectors* of length $N_1 \equiv N + 1$:

$$[R] = [R_{i,N_1}] = \begin{pmatrix} R_{1,N_1} \\ R_{2,N_1} \\ \vdots \\ R_{N_1,N_1} \end{pmatrix}, \quad (1.50)$$

$$[V] = [V_{i,N_1}] = \begin{pmatrix} V_{1,N_1} \\ V_{2,N_1} \\ \vdots \\ V_{N_1,N_1} \end{pmatrix}. \quad (1.51)$$

The integral equation (1.49) can be rewritten as the matrix equation:

$$[F][R] = [V], \quad (1.52)$$

$$F = 1 - DV, \quad \Rightarrow F_{ij} = \delta_{ij} - D_j V_{ij}, \quad (1.53)$$

With R the unknown vector, (1.52) is in the standard form $AX = B$, which can be solved by use of mathematical subroutine libraries.

1.2.9 Solution via Inversion or Elimination

An elegant (but alas not most efficient) solution to (1.52) is by direct matrix inversion:

$$[R] = [F]^{-1}[V], \quad (1.54)$$

where the computers performs the inversion numerically. Because the inversion of even complex matrices is a standard routine in mathematical libraries, (1.54) is a *direct solution* for the R matrix. A more efficient approach is to find an $[R]$ that solves $[F][R] = [V]$ without computing the inverse. This is accomplished by Gaussian *elimination*.

Subroutine Name	Description
LPOTT	Main program; begins execution, read in data, setup
Beslia	Spherical Bessel functions of imaginary argument
CGc2	Square of Clebsh Gordon coefficients
FFact	Nuclear Form Factor
FFX	Form Factors for ^3He and ^3H
Ffpn	Form Factor for proton and neutron
Gauss	Gaussian integration points
HarmNuc	Gaussian form factor for harmonic oscillator nuclei
Lagrng	Lagrange interpolation
LogPlt	Semilogrithmic plot on printer
LegPol	Legendre polynomials
Minv	Matrix inversion
mixup	Mixes partial waves when transform reference frames
OptP	Computes optical potential
Plprme	Derivative of Legendre polynomial
rcwfn	Coulomb Wave function in coordinate space
rhok, rhokff, rhoofr	Nuclear form factors and densities
sigcl	σ_c , the pure Coulomb phase shift
spBesl	Spherical Bessel function
Tfold	Fermi averaging (folding)
Tncm, Tnoff	On & off-shell πN amplitudes in πN COM
Tnuc, Tnucth	πN amplitudes in $\pi\text{Nucleus}$ COM
Tpirsl	Rowe, Saloman, Landau πN amplitudes
Vabs	True π absorption potential
Vcoul, Vc	Coulomb potential
WavFn	π -nucleus wave function

Table 1.1: The subroutines of LPOTT and their general purposes. You should compile all subroutines.

1.3 Simulation: Get LPOTT Running

In the directory/folder LPOTT is everything you need to run the program, including some sample cases. Here you will find the subdirectories that LPOTT uses for research:

```

LPOTT  Directory and main program name
Subs   Fortran subroutines
In     input data files, sample control files
Out    named output files
Run    script to assemble and run program

```

1.3.1 Compiling

The input data files are in the subdirectory `in`, and the output files produced by LPOTT are in `out`. The script file `run` (for Unix) attends to the input and output files, as well producing information about the run. For non-Unix systems, you might want to set up a similar script. We usually give a descriptive name to the input files, such as `He3`, and place it in the subdirectory `in`. The program then automatically produces an output file of the same name in the directory `out`.

1. Go to `subs` and compile all the subroutines there. The subroutine that should be there and their purposes are indicated in Table 1.1.
2. Store the executable `a.out` in the file `Lpott`. If you use the `-o Lpott` option to the compile command, this is done automatically. You can leave the executable in the file `a.out` and use that name instead of `Lpott` in what follows, but things can then get confusing since you cannot tell one `a.out` from another.

3. Move the executeable `Lpott` to your own, personal, working directory.
4. In order to get a feel for how to execute LPOTT, run through the following steps by hand. Use the `run` command, which does all this for you, for subsequent executions.
5. The input files have the historical names of `tapeN`, $N= 1, 4$. Set up the four input tapes by copying files from the `in` directory to them:
 - `in/dela1` (input πN phase shifts) to `tape1`
 - `in/gth` (input πN potentials) to `tape2`
 - `in/talnf` (input πN T matrices) to `tape3`
 - `in/denc1` (input πN denominator) to `tape4`
6. Run the program with the input control parameters from `in/sample` and with the output going to `out/sample`:


```
Lpott < in/sample > out.sample
```
7. Check that the file `out/sample` has been created and that it agrees with the files `out/sample.bak` (reproduced below).
8. If there are significant differences, then something is wrong. See if you can fix it. If not, ask your instructor for help. If no one can fix the problem, try contacting the authors.
9. Try modifying the script `run` so that a version of it will run on your system. For example, execute it with

```
run Lpott sample
```

1.3.2 Understanding the Output

The output file should contain a great deal of information that chronicles all the steps that LPOTT has gone through during the calculation. Make sure to look at the top of the output since it tells you what LPOTT thinks you have told it to do via the `in/sample` file. As with other complicated programs, always check that LPOTT is running the case you want (“garbage in, garbage out” as they say). The sample output looks like this:

```

program= Lpott input= in/sample Tue Jan 1 12:30:30 PST 2002
$pi$-nucleus scattering via lpott (CPlab 2002 version), orig 1/86
ok tape6
 1 10
50.0000
16 22 0.20E+05 3-2.00-3.00
no of grid points= 16
 1.5500 1.5500 0.0000 1.5500 1.5500 0.0000 3.0000 7.0000
 6 12 0 101705003 0 0 0 0 0 0 0 0 0 0
nifty( 1)= 0 pi+ nifty( 2)= 1 *5=be shift
nifty( 3)= 0 no w.f. nifty( 4)= 1 nlsp-g(p)
nifty( 5)= 7 e3b, aay nifty( 6)= 0 no spin ms
nifty( 7)= 5 abs-old,sp nifty( 8)= 0 nifty( 9)= 0
no Pauli nifty(10)= 3 exact coul nifty(11)= 0
pi0,pi-,k+ shift nifty(12)= 0 pi+,ko shift nifty(13)= 0
pi-channel shift nifty(14)= 0 pi+channel shift
nifty(15)= 0 not used shift nifty(16)= 0
rhog,rho2g nifty(17)= 0 kmt nifty(18)= 0 full
amps plt(19)= 0 use nif-16 nifty(20)= 0 no
t10 plt nes,nwaves,b0r,b0i,c0r,c0i= 59 14 0.00000 0.00000
0.00000 0.00000 nes,nwaves,b0r,b0i,c0r,c0i= 59 14 -0.04000
0.04000 0.00000 0.08000
***** amass= 12.0000*****

tpi epilab ecm(Sqrts) kcm plab
50.0000 189.5780 11447.9312 126.1716 128.2880

relativistic calculation

energy momentum
50.0000 126.1716

---- angular momentum = 0----

opt poten values for kp=k0= 126.172and l=1
k rev vc rabs(n0 flip) rabs(flip)imv imvabs(noflip),imabs(flip)

```



```
eof in main
```

Here the lines up to `*** amass= 12` are an unprocessed printout and explanation of the input data you have given LPOTT in file `in/sample`. After the `amass` printout, LPOTT prints out some kinematics quantities, such as energy and momentum, and tells you whether you called for a relativistic or nonrelativistic calculation.

Next LPOTT loops through all the partial waves, and computes the R and T matrices for each l value. Since the — **angular momentum = 0** case is the first, at this point a number of quantities must be computed that will also be stored and used for higher angular momenta as well. After the printouts of the partial-wave T matrices, the differential cross sections and total cross sections are printed out, as well as some printer plots of the differential cross sections (the code was written before the advent of graphical terminals).

1.3.3 Understanding the Logic: Follow the Data Flow

A good approach for developing some feel of how a complicated program works is to follow the flow of data through it. You have just ran the sample case and generated output that looks right. In Table 1.1 we gave you a list of all the subroutines in LPOTT, not all of which get used every time.

Start with the data file used by this sample run and trace its flow through the subroutines. To do that you need a paper or electronic listing of the program. Then make a list, starting at `main`, that gives the names of the subroutines called by LPOTT for these input parameters. Use Table 1.1 to add the description of each subroutine, and thereby chronicle the logical flow through the program.

Alternatively, make a flow chart by using arrows to show which subroutine calls which other ones. With this scheme you need only list each subroutine once and you get a visual picture of the logic.

1.4 Experiments

1.4.1 Experiment 1: Checking the Input πN Scattering

When faced with a big and complicated program like LPOTT, a good start is to understand some of the important parts that comprise the package. If they do not work as expected, then either you need to understand more or fix something that may be broken.

For LPOTT, the physics is the optical potential (1.36) or (1.37). We see from these expressions that the potential is simply the product of the πN T matrix and the nuclear density ρ . Since the most dynamic part of the optical potential arises from the πN T matrix elements, in this first simulation we will explore the elementary πN T matrix elements that are used as input to the optical potential.

Exercise 1: The πN Phase Shifts

Browse through the file `delta_al` in the `in` subdirectory (the “al” indicates that these phases were collected by Almehed and Lovelace [AL]). For each value of 71 values of the πN COM energy E_{COM} , you should find a πN absorption parameter η_l and a phase shift δ_l , for each of 14 partial waves. The COM energy is given by (1.2), which has the minimum value

$$E_{COM} = \sqrt{m_\pi^2 + \kappa^2} + \sqrt{m_N^2 + \kappa^2} > m_\pi + m_N \simeq 1078 \text{ MeV}, \quad (1.55)$$

E_{COM} is seen to start at about 200 MeV above the sum of the masses.

Since the πN system has spin and isospin, what we call “waves” here, and `nwaves` in the code, are actually a combination of orbital angular momentum, spin, and isospin which is

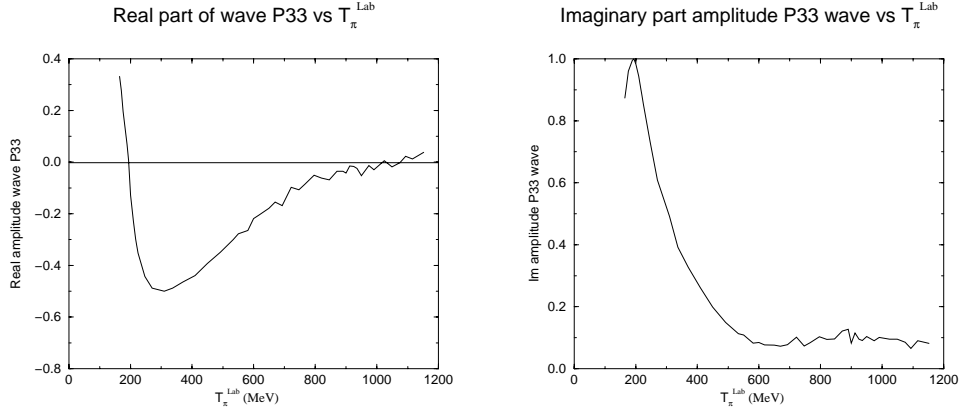


Figure 1.7: (*left*) Real part and (*right*) imaginary part of the P33 πN partial wave amplitude.

denoted by the symbol $L_{2I,2J}$. As indicated in the subroutine `tncm.f`, the `nwave` code is

nwave	$L_{2I,2J}$	nwave	$L_{2I,2J}$	nwave	$L_{2I,2J}$	nwave	$L_{2I,2J}$	nwave	$L_{2I,2J}$
1	s31	2	p31	3	p33	4	s11	5	p11
6	p13	7	d33	8	d35	9	f35	10	f37
11	d13	12	d15	13	f15	14	f17		

If you try to run LPOTT at an energy below the lowest of that in the file of phase shifts, it will use an analytic function that Rowe, Salomon and Landau fit to the low energy phase shifts. Look at the subroutine `Tpirs1` in the `subs` directory and check through the sections which compute the phase shift and the T matrix. Plot the input P33 (`nwave =3`) phase shift as a function of energy. It should rapidly pass through 90° at a COM energy of about 1238 MeV.

Exercise 2: The P33 Argand Plot

In the `subs\Testroutines\Fortran` directory we have placed a program `TestPiNdel.f` that computes the elementary, input πN T matrices. This is the type of program a researcher might write to test individual pieces of a big program. `TestPiNdel.f` reads πN phase shifts from the file `delal`, augments it with lower-energy phases from `tpirs1.f`, and then calls `argand.f` to compute the real and imaginary parts of the partial amplitude (1.25),

$$T_l = \frac{1}{2i} (\eta_l \exp 2i\delta_l - 1). \quad (1.56)$$

The results for just one partial wave (`nwave=3`, P33) are stored in `TestPiNdel.dat` for you to plot up with your favorite graphics program.

1. Make a plot of the real and imaginary parts of the P33 πN scattering amplitude as functions of energy, as we have done in Fig. 1.7. Record the energy at which the real part vanishes and at which the imaginary part is maximum. This is the resonance energy.
2. Make an Argand plot of the P33 πN wave.
3. Add a circle of radius 0.5 and centered at $(0,1/2)$ to your Argand plot and check if the resonance is elastic.

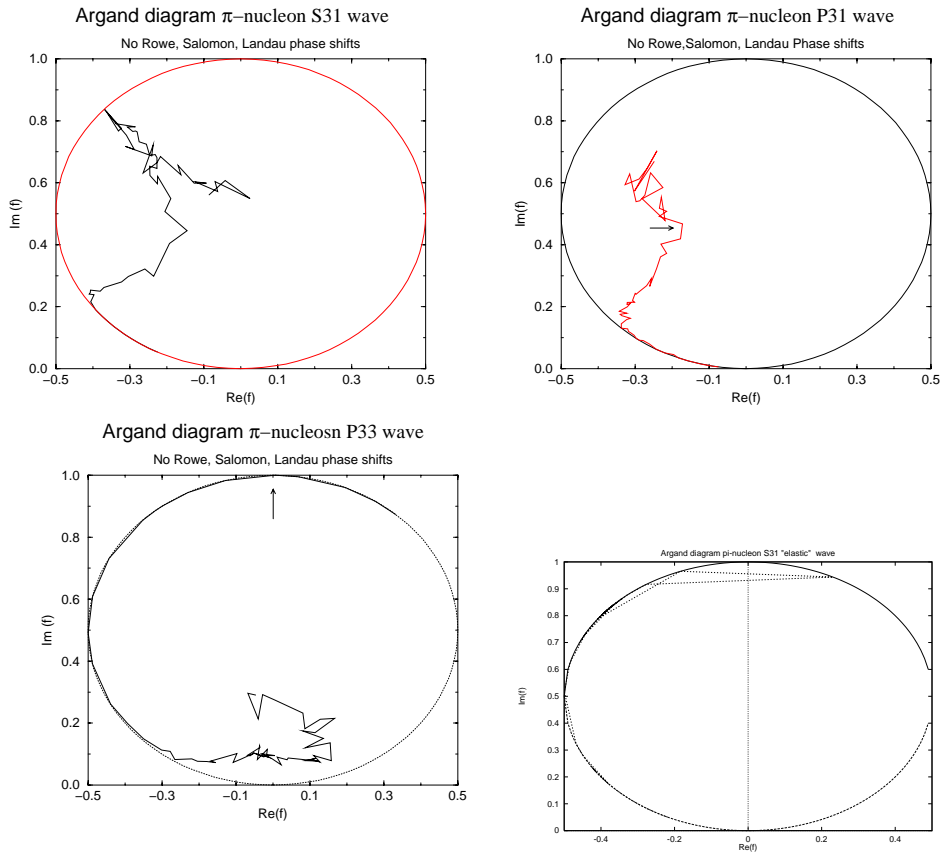


Figure 1.8: *Reading from upper left:* The Argand diagrams for S31, P31, P33, and purely elastic S31 partial waves. Note that the purely elastic scattering lies on the circle.

4. Deduce whether increasing energy corresponds to clockwise or counterclockwise motion.
5. In Fig. 1.8 we give the Argand diagrams for the P33 partial wave using only the higher-energy phase shifts. Your P33 case should be similar. Compare your Argand plot to the separate plots of the real and imaginary parts of the scattering amplitude and correlate the behaviors.
6. Extract from your Argand plot the energies for which $\text{Im}f_{P33} = 1/2$. The difference in these two energies is the *full width at half maximum*.

Exercise 3: Other πN Waves

Make Argand plots of other partial waves and search for resonances in them too. We give some samples in Fig. 1.8, where you will note considerable inelasticity.

Exercise 4: πN Total Cross Sections

Included in the file `TestPiNdel.f` is the subroutine `crosssect.f` that computes the πN total cross section as a function of momentum according to (1.28).

1. Modify `TestPiNdel.f` so that cross sections are now outputted to `TestPiNdel.dat`.

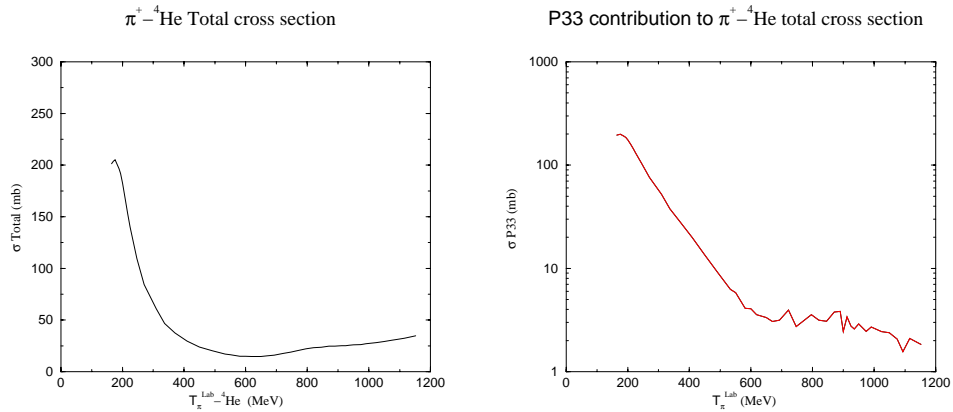


Figure 1.9: The energy dependence of the elementary π -proton (*left*) and π -neutron (*right*) total cross sections.

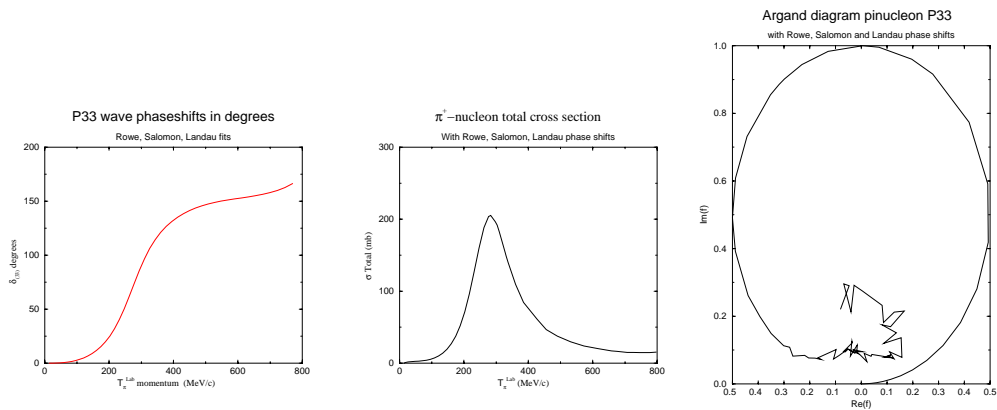


Figure 1.10: The energy dependence of the P33 $\pi - N$ interaction containing a resonance. (*Left*): phase shift δ_{33} , (*center*): total cross section, (*right*): Argand diagram.

2. Run the edited code and plot the total cross section for the P33 wave as a function of energy.
3. Compare your plot to the one in Fig. 1.9. Record the pion kinetic energy and momentum at which there is a resonance peak.
4. Decide if the total cross section resonance occurs at the same energy as the scattering amplitude in the Argand plot.

1.5 Experiment 2: Low-Energy $\pi - {}^4\text{He}$ Scattering

The file `sample` in the `in` directory was for π scattering from a ${}^{12}\text{C}$ nucleus. Copy that file to a new one named `He4` and modify it so that it supplies the parameters needed for $\pi^- - {}^4\text{He}$ scattering (${}^4\text{He}$ has $Z = 2$ protons and $A = 4$ nucleons). The top of the listing of the main program `LPOTT.f` explains the nifty values. Here is a good set of input:

1 10	nr (1 for relativistic), 10 π -A partial waves
110.0	π kinetic energy in lab
16 22 20000. -3 -2. -3	1 st 3 numbers control integration, last 3 plotting
1.362 0.316 0.00 1.362 0.316 0.00 3.0 7.	Radii of nuclear densities
2 4 0 1 0 1 7 0 5 2 0 3 0 0 0 0 0 3 0 0 0 0 0 0 0	Z, A, 20 Nifty's
59 14 0. 0. 0. 0	# of π N energies and partial waves; b_0, c_0

Now run a series of simulations to examine the effect on scattering of changing the incident pion's kinetic energy and charge. Since the nucleus is positively charged and the π can have positive or negative charge, both the nuclear and Coulomb force contribute to as described by (1.30).

Repeat part of the 1978 calculation of Landau and Thomas [LT] which explained some baffling experimental results. In that work they discovered that for low energies, the strong force on the π arising from the nucleus becomes unusually weak. Accordingly, the Coulomb force, which is normally expected to be much weaker than the nuclear force, except for very small scattering angles, interferes strongly with the nuclear force at large scattering angles.

The Coulomb-nuclear interference arises from destruction or construction when summing the real parts of the Coulomb and nuclear amplitudes. Regardless of the sign convention (our's has positive potential causing negative real amplitude), the real parts will have the same sign, and thus interfere constructively, if both forces are either attractive or repulsive; if one is attractive and the other repulsive, there will be destructive interference. Since the π^+ and π^- mesons have the same nuclear force but opposite electric charge, one meson will experience constructive interference while the other will experience destructive interference. You will have to experiment to see which meson does what!

1. Run LPOTT for both π^+ and π^- scattering at 50 MeV from ^4He . This corresponds to two different values of `Nifty(1)`.
2. While the Coulomb force is independent of energy, the nuclear force depends sensitively on the energy. As indicated above, the nuclear force essentially vanishes at some energy and so you should try a number of energies and see how the scattering varies. Run the program for (at least) π laboratory kinetic energies of 24, 30, 40, 50, 75 and 110 MeV.
3. Look at each output file produced by each run. In the section before the printer plots you should see a table of the predicted differential cross sections. It has a title beginning with:

```
th-c.m.  cos(cm)  dsig/dw-cm  ds/dw(b.a.)  t  th-lab  .....
```

4. We are interested in the first and third columns. The first column gives the scattering angle θ in the center of mass system that the outgoing π makes with the incident beam. The third column gives the differential cross section $\frac{d\sigma}{d\Omega}$ in mb units.
5. Extract these two columns from the output and use your favorite plotting program to draw a semilogarithmic plot of the differential cross section versus θ . Place the plots for all the energies on the same graph. Your plot should look something like Fig. 1.11.
6. Repeat these same calculations for these same energies but now for the scattering of a negative π from ^4He .
7. Observe the differences between the computed cross sections for π^+ and π^- scattering, especially for small scattering angles, and conclude which has destructive and which has constructive interference.

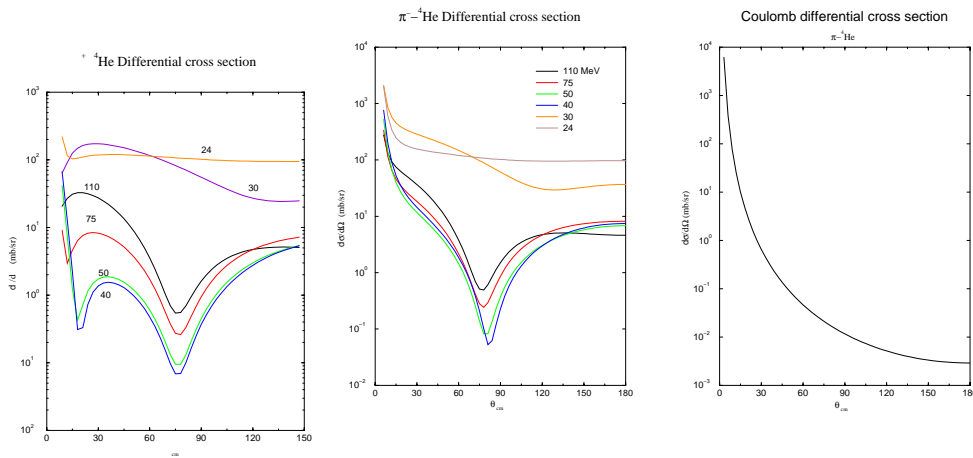


Figure 1.11: Differential cross sections at several incident π energies for (left) π^- , (center) π^+ , and (right) pure Coulomb scattering from a ${}^4\text{He}$ nucleus.

The right part of Fig. 1.11 shows the differential cross section that results when a positive π is scattered by just the repulsive Coulomb potential of the ${}^4\text{He}$ nucleus. Of course this could not occur in nature unless the master of the universe and could somehow turn off the nuclear force, but it does lead to an interesting theoretical comparison. In general, we expect that interference can occur when the pure Coulomb and pure nuclear cross sections are of comparable magnitude.

To understand how the nuclear and Coulomb forces interfere with each other, we note that a π^+ meson always feels a repulsive Coulomb force due to the positively charged nucleus. If the nuclear force is also repulsive, then there will be constructive interference and the cross section will always be larger than the pure Coulomb cross section⁴. If, on the other hand, the nuclear force is attractive, then there will be destructive interference and the cross section will dip below the pure Coulomb cross section.

In left hand part of Fig. 1.11 we see a minimum in the cross section at $\theta \simeq 12^\circ$ followed by a maximum at about $\theta \simeq 40^\circ$ for all energies above 30 MeV. This is due to the destructive interference, and tells us that since the Coulomb force is repulsive, the nuclear force must be attractive. As the energy decreases from 110 MeV, the minimum moves out in angle and at $T_\pi=30\text{MeV}$, the Coulomb minimum merges with the minimum caused by the large πN P wave at $\simeq 70^\circ$. At 24 MeV, the interference minimum vanishes completely and the cross section rises; this is due to sign change in the real part of the nuclear amplitude. In contrast, note how the $\pi^- - {}^4\text{He}$ scattering, which always has constructive interference, shows a monotonic decrease with energy.

1.6 Experiment 3: Pion-Nucleus Total Cross Sections

We have seen in Fig. 1.10 and Section 1.4.1 that the elementary πN interaction exhibits a resonance in the P33 partial wave. The question you now investigate is “Does this resonance still exists when the π scatters from a nucleus, which is, after all, composed of nucleons?”

We look at $\pi^+ - {}^4\text{He}$ scattering for the answer.

1. Examine the output you already have for $\pi^+ - {}^4\text{He}$ scattering and extract from it the data for the $\pi^+ - {}^4\text{He}$ total cross section as a function of π kinetic energy.

⁴Actually the argument is more complicated than this because the complex scattering amplitudes must be added together before squaring to form the cross section, but we will ignore such complications here.

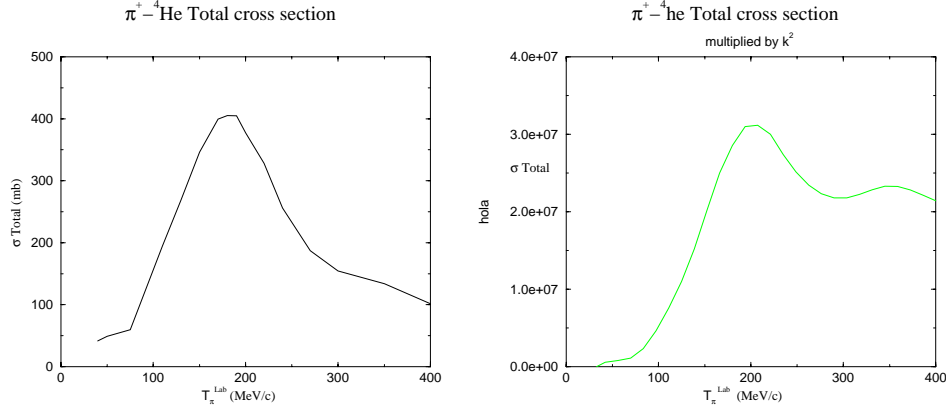


Figure 1.12: (*left*) The total cross section as a function of energy for pure nuclear π scattering from a ${}^4\text{He}$ nucleus; (*right*): the total cross section times the π 's momentum squared k^2 .

2. Plot your total cross sections. You should get a plot similar to that on the left of Fig. 1.12.
3. Record the π lab kinetic energy at which the $\pi^+ - {}^4\text{He}$ total cross section has a peak.
4. Record the π lab kinetic energy at which the $\pi^+ \text{N}$ total cross section has a peak.
5. If both of these peaks occurred at the same energy, it would be quite reasonable to believe that the peak in the $\pi^+ - {}^4\text{He}$ total cross section is due to the P33 resonance. However, the energies differ (record which is higher) and so things are not so simple. One possible explanation is that the shift in peak position is due to some kinematic, rather than dynamic, effect. For example, equations (1.9) and (1.28) that relate the total cross section to phase shifts take the simple form for spinless particles of

$$\sigma^{\text{tot}} = \frac{4\pi}{k^2} \sum_l (2l+1) e^{i\delta_l} \sin(\delta_l), \quad (1.57)$$

where we have set the inelasticity $\eta_l = 1$ for clarity. We know that the π -N resonance occurs when the phase shift $\delta_l = \pi/2$, at which point $\sin \delta_l$ has a maximum. However, the $1/k^2$ factor will shift the peak in the total cross section downwards since this factor is larger at small k than large k .

6. To see if such a kinematic effect is shifting the peak in the $\pi - {}^4\text{He}$ total cross section, multiply your total cross section data by k^2 and plot those up as a function of kinetic energy (this is what we have done on the right of Fig. 1.120).
7. Record the change in peak position arising from the $1/k^2$ factor and comment on the agreement with the simulation.
8. Another way that the nuclear environment may influence the effect of the elementary πN resonance is through multiple scattering. By this we mean that there are a number of nucleons within a nucleus and that these nucleons are moving (much like the Fermi distribution of electron energies within a metal). Accordingly, there is not one precise energy at which the incident π interacts with each N, but rather a spread of values for the π -N effective energy. And if the resonance is spread out, then the $1/k^2$ factor will shift it up further in energy.
9. To test if the multiple scattering of the π by the nucleons within the nucleus is causing the total cross section peak to broaden and consequently shift, repeat the analysis of

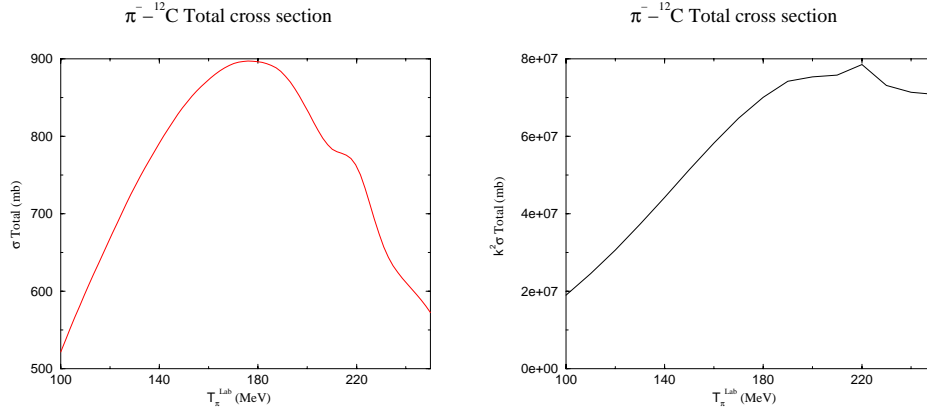


Figure 1.13: (*left*) The total cross section as a function of energy for pure nuclear π scattering from a ${}^{12}\text{C}$ nucleus; (*right*): the total cross section times the π 's momentum squared k^2 .

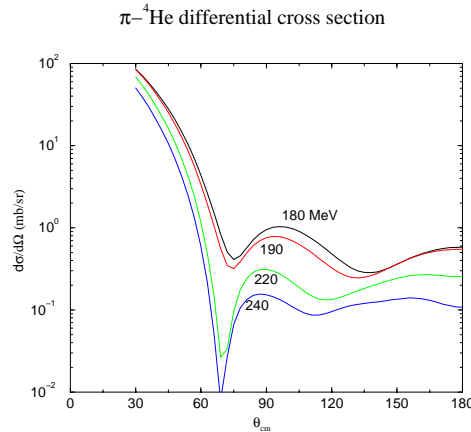


Figure 1.14: Differential cross sections for π scattering from an unpolarized ${}^3\text{He}$ nucleus at a number of energies.

total cross sections you just did for ${}^4\text{He}$ now for ${}^{12}\text{C}$. Since carbon has three times as many nucleons as does helium, the shift should be larger. Your results should look somewhat like Fig. 1.13, originally investigated by [LPT].

1.7 Experiment 4: P33 Resonance in $\pi^- - {}^{12}\text{C}$ Scattering

Now that we have seen the influence of the πN P33 resonance on total cross section we may ask “what is the resonance’s effect on the differential cross sections?” There are a number of ways to answer this and we shall use our simulations to provide some answers.

1. From a qualitative point of view, we might say that since the elementary π -N resonance is in the P wave ($l = 1$), we would expect there to be a large P wave contribution to π -nucleus scattering. As follows from the partial-wave expansion of the scattering amplitude, (1.25), a large $l = 1$ contribution would mean a large weighting factor for $P_1(\cos\theta)$ Legendre polynomial. Yet since $P_1(\cos\theta) = \cos\theta$, this would lead us to predict that the differential cross section behaves like $\cos^2\theta$, that is, with a peak in the forward direction and a deep minimum near 90° .

- Look at the plots and data for your π - ^4He differential cross sections in the COM system and note the deep minimum near 90° for energies near resonance ($T_{lab}^\pi \simeq 180$ MeV).

We got the cross sections in Fig. 1.14 with the input:

```

      1  10
      240.0
    16 22 20000.   -3  -2.  -3.
    1.362   0.316   0.00   1.362   0.316   0.00   3.0   7.
      2   4   0  1  0  1  7  0  5  2  0  3   0  0  0  0  0  3   0  0  0  0  0  0  0
      59  14  0.  0.  0.  0.

```

- Record the angle at which the minimum occurs in the differential cross section for π - ^4He scattering.
- Examine the differential cross sections for π scattering from the ^{12}C nucleus in the COM system for energies near resonance and record again the angle at which there is a minimum in the differential cross section.
- You should be finding that for π scattering from both helium and carbon, the minimum in the differential cross section occurs at a *smaller* angle than the 90° for which it occurs for scattering from a single N. The reason for this is kinematic; the 90° angle is in the π -N COM system, while we have been looking at the cross sections in the π -nucleus COM. Since the nucleons in the nucleus are essentially at rest, a transformation from the π -N to π -nucleus COM would push the entire differential cross section forward in angle, what is known as the “beacon effect”.
- To gauge how large this beacon effect is, consider π N scattering at 180 MeV kinetic energy and at a COM scattering angle of 90° . Compute the corresponding scattering angle in the lab system. The kinematic relation is

$$\tan \theta_{lab} = \frac{\sin \theta}{\cos \theta + m_\pi/m_N}. \quad (1.58)$$

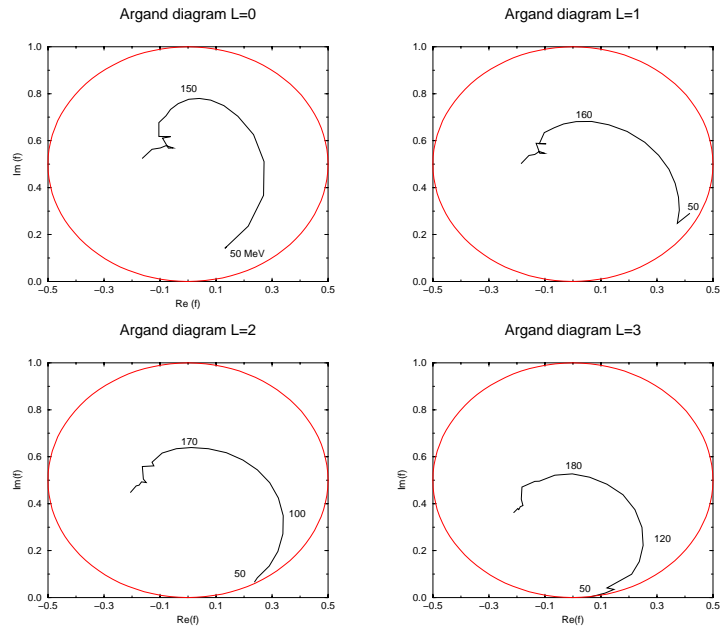
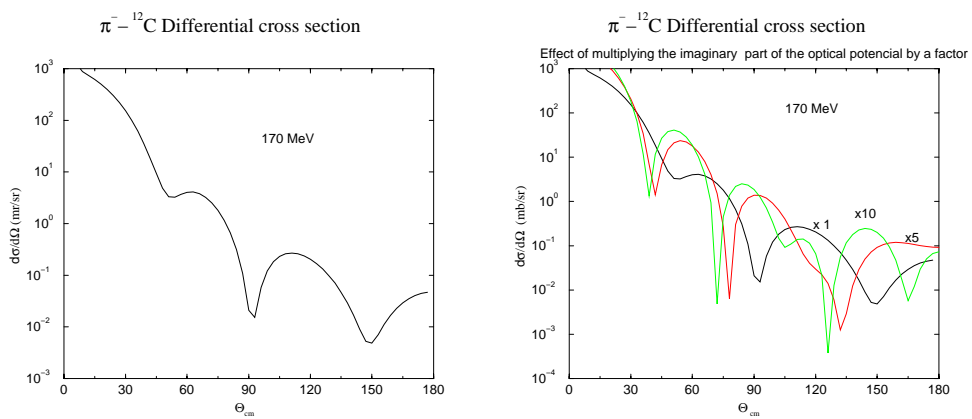
Is this the right size to explain the shift in the angular position of the resonance?

- A more reliable way to determine if a resonance is present is to make Argand plots for individual partial waves. If you look back at Fig. 1.4 and the P33 part of Fig. 1.8, you will notice that the Argand plot makes a counter-clockwise loop as the energy passes upwards through resonance. If there is some P33 signal present in π -nucleus scattering, then the π -nucleus Argand diagrams should have these types of loops in them.
- Take your output for π scattering from some nucleus and plot Argand diagrams up showing the partial wave amplitudes T_l as a function of energy for $l = 0 \dots 3$. Do you see evidence of resonances? Some of our results for π -carbon scattering are shown in Fig. 1.15.

1.8 Experiment 5: Make a Nucleus Black

As we discussed before, the optical potential gets its name from the similarity of light scattering and particle-nucleus scattering. We know that if light scatters from a completely absorptive or “black” disk or sphere, a characteristic diffraction pattern with sharp minima and maxima results.

LPOTT uses a complex potential to model the interaction of the π with the nucleus. The imaginary part of this potential is responsible for the absorption of the π as it travels through the nucleus. In this simulation you will make the nucleus successively blacker by successively increasing the imaginary part of the optical potential.

Figure 1.15: Argand diagram for $\pi^- - {}^{12}\text{C}$ scattering in the partial waves: $l = 0 \dots 3$.Figure 1.16: (*Left*): the $\pi^- - {}^{12}\text{C}$ differential cross section at 170 MeV; (*right*): the effect of increasing the “blackness” of the nucleus obtained by multiplying the imaginary part of the potential by factors of 5 and 10.

- To maximize the blackness of the nucleus, we want an energy near resonance which maximizes the imaginary part and minimizes the real part of the optical potential. A good choice is 170 MeV.
- A nucleus like ${}^4\text{He}$ may be too small to absorb a good amount of the incident beam, and so try a nucleus at least as large as ${}^{12}\text{C}$. Appropriate input parameters for $\pi^- - {}^{12}\text{C}$ are

```

      1  10
      170.0
      16 22 20000.   -3  -2.  -3.
      1.55   1.55   0.00  1.55   1.55   0.00  3.0 7.
      6   12  1  1  2  1  7  0  5  2  0  1  0  0  0  0  0  0  0  0  0  0  0  0  0  0
      59  14  0.  0.  0.  0.

```

- The optical potential is calculated in the subroutine `optp.f`, and so you need to go in there and make the imaginary part of the optical potential bigger by factors of 5, 10, and 100.
- Now look through `optp.f`. Since the matrix manipulation routines available at the time LPOTT was written could handle only real matrices, the single matrix equation (1.49) using complex matrices was converted to two simultaneous equations using real matrices. In addition, to speed up what at the time was very expensive calculations, the matrices were stored in a linear form (one lone vector).
- The fragment of `optp.f` below shows the place where the matrix elements of optical potential are assigned. You need only modify the line with the following exclamation sign (the spin-independent case):

```

      npot1 = (i2-1)*n2+i1
320      npot2 = npot1+n1*(n2+1)
      npot3 = npot2-n1
      npot4 = npot1+n1
      u(npot1,1) = f(npt,1)
      u(npot2,1) = u(npot1,1)
      u(npot3,1) = f(npt,2) * 10.0 ! to see blackness
      u(npot4,1) = -u(npot3,1)
c      spin-dependent potentials

```

- Fig. 1.16 shows the effects of multiplying the imaginary part of the optical potential by factors of 5 and 10 to make it more black (absorptive). The original differential cross section is also shown. You should obtain similar results.
- Now experiment with making your blackest nucleus *bigger*. If the scattering is really like a black disk, this should cause the entire diffraction pattern to shrink into smaller angles and get sharper. The size of the nucleus is controlled by the four 1.55 parameters above (they are the size in fm's). Just increase them all to see the effects.

1.9 Reprints of Original Papers

Bibliography

- [AL] S. Almeded and C. Lovelace[AL], Nucl. Phys. B40 (1972) 157.
- [QMII] R.H. Landau, *Quantum Mechanics II*, (1996) Second Edition, Wiley-Interscience, New York.
- [Tri-78] R.R. Johnston, T. G. Masterson, K.L Erdman, A. W. Thomas and R.H. Landau, Nucl. Phys. **A296** (1978) 44-460.
- [KMT] A.K. Kerman, H. McManus, and R.M. Thaler, Ann. of Phys/ **8**, (1959) 551.
- [Koltun] Judah M Eisenberg and E S. Koltun, (1980), Theory of meson interactions with nuclei, Wiley-Interscience, New York.
- [Hadj] C. Hadjimichael, B. Goulard and R. Bornais, Phys. Rev. C **27**, (1983), 831.
- [LT] R.H. Landau and A.W. Thomas (Nucl. Phys. A **A302** (1978) 461-492).
- [LPOTT] R.H. Landau, Comput. Phys. Commun. **28** (1982) 109.
- [LPT] R. H. Landau, S. C. Phatak, and F. Tabakin, Ann. Phys., **78** (1973), 299, and for similar results with Oxygen, see S.C. Phatak and F. Tabakin Phys. Rev. C **7** (1973) 1803.
- [RSL] G. Rowe, M. Salomon and R.H. Landau, Phys. Rev. C **18** (1978) 445.
- [Yuk35] Yukawa., and K. Chihiro, *Birth of the Meson Theory.*, Am. J. Phys., **18** (1960) 154.